Pump-Induced Temporal Contrast Degradation in Optical Parametric Chirped-Pulse Amplification: Analysis and Experiment

Introduction

Laser–matter interactions in new regimes have occurred due to the generation of high-intensity optical pulses using large-scale laser systems.[1] The interaction regime of a laser pulse with a target is basically set by the peak intensity of the pulse, which is fundamentally proportional to the ratio of the pulse energy to the duration of the pulse and surface of the focal spot. Intensities of the order of 10^{22} W/cm^2 have been claimed,[2] and facilities delivering high-energy, high-intensity laser pulses are under operation or construction.[3] The interaction can be detrimentally impacted by light present before the main pulse since absorbed light can lead to physical modification of the target.[4] The temporal contrast of a laser pulse is the ratio of the peak power of the main pulse to the power of the light in some predetermined temporal range before the main pulse. The contrast can be reduced significantly during the generation and amplification of laser pulses, and contrast degradation manifests itself as isolated prepulses or as a slowly varying pedestal. Incoherent laser and parametric fluorescence can significantly impact the contrast of laser pulses and can lead to a long-range pedestal on the recompressed pulse.[4,5] This contrast degradation is fundamental since fluorescence is always present for classical optical amplifiers. The contrast of optical parametric chirped-pulse amplifiers, however, is also detrimentally impacted by temporal variations of the intensity of the pump pulse that induce spectral variations on the stretched amplified signal via the instantaneous parametric gain. This is a practical limitation that can be eliminated or reduced by proper design of the pump pulse and the optical parametric chirped-pulse amplification (OPCPA) system.

The parametric gain induced by a pump pulse in a nonlinear crystal is an efficient process for large-bandwidth, high-energy amplification of chirped optical pulses.[6–8] It is used in stand-alone systems[9–16] or as the front end of large-scale laser facilities.[17] The impact of temporal fluctuations on the contrast of the recompressed signal in an OPCPA system was first identified by Forget *et al.*[18] Simulations of the effect of pump-pulse amplified spontaneous emission (ASE) on an OPCPA system have linked the ASE coherence time to the temporal extent of the induced pedestal.[19] These publications offer a physical explanation of pump-induced contrast degradation, but an analytical treatment is necessary to quantify the impact of this phenomenon, improve the contrast of existing systems, and design new high-contrast OPCPA systems. This article quantifies the impact of incoherent pump-pulse ASE using an analytic formalism for pump-induced temporal contrast degradation in OPCPA systems and presents an experimental solution to reduce this impact. The impact of incoherent pump ASE is analytically quantified as a function of the operating regime of the OPCPA system. The following sections (1) present the necessary formalism and derive general equations describing the pump-induced contrast degradation in OPCPA systems; (2) compare these analytical derivations with simulations, bringing to light the magnitude of these effects in a typical OPCPA system; and (3) describe an LLE experiment that demonstrates the reduction of pump-induced temporal contrast degradation by filtering the pump pulse with a volume Bragg grating (VBG) in a regenerative amplifier.

Analysis of Pump-Induced Contrast Degradation in an OPCPA System

1. General Approach

The derivations presented in this section assume a one-dimensional representation of the electric field of the signal and pump as a function of time (and equivalently optical frequency), without spatial resolution. Such a model is sufficient to introduce the various aspects of contrast degradation in OPCPA systems. Some of these systems use flattop pumps and signals, in which case the temporal contrast is mostly limited by the contrast obtained in the constant-intensity portion of the beam. For high energy extraction, efficient phase matching, and optimal beam quality, OPCPA systems are usually run in configurations where spatial walk-off and diffraction are not significant. An instantaneous transfer function between the intensity of the pump, the intensity of the input signal, and the intensity of the output signal is used to describe the parametric amplifier. This applies to an amplifier where temporal walk-off and dispersion-induced changes in the intensity of the interacting waves are small compared to the time scales of the temporal variations of the signal and pump. This also applies to a sequence of amplifiers where scaled versions of the same pump are used in each amplifier with an identical relative delay between the signal being amplified and the pump. Figure 111.1 presents a schematic of an OPCPA system. The short input signal is stretched by a stretcher, amplified by the pump pulse in an optical parametric amplifier (one or several nonlinear crystals properly phase matched), and recompressed. As identified in Refs. 18 and 19, the variations of the parametric gain due to variations in the pump intensity lead to modulations of the temporal intensity of the amplified stretched pulse, which are equivalent to modulations of the spectrum of this pulse. These modulations lead to contrast-reducing temporal features after recompression.

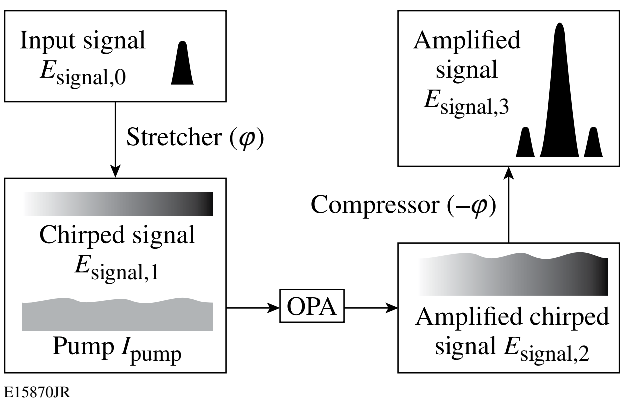

Figure 111.1
Schematic of an OPCPA system. Pump-intensity modulation gets transferred onto the spectrum of the chirped signal in an optical parametric amplifier (OPA). The modulation of the spectrum of the recompressed signal induces contrast-reducing temporal features on the recompressed signal.

2. Contrast Degradation of an OPCPA System in the Presence of Pump Noise

In this article, E and $\tilde{E}$ relate to the temporal and spectral representations of the analytic signal of an electric field, and I and $\tilde{I}$ relate to the corresponding intensities. The initial signal is described by the spectral field $\tilde{E}_{\text{signal},0}(\omega)$. After stretching with second-order dispersion φ, the stretched pulse is described in the time domain by

$$E_{\text{signal},1}(t) = \left(1/\sqrt{\varphi}\right)\tilde{E}_{\text{signal},0}(t/\varphi)\exp\left(-it^2/2\varphi\right)$$

up to some multiplicative constants. The quadratic phase describes the one-to-one correspondence between time and optical frequency in the highly stretched pulse, which is symbolically written as $t = \varphi\omega$. The temporal intensity of the signal after parametric amplification is a function of the temporal intensity of the stretched signal $I_{\text{signal},1}(t) = (1/\varphi)\tilde{I}_{\text{signal},0}(t/\varphi)$ and the temporal intensity of the pump $I_{\text{pump}}(t)$, which can be written as

$$I_{\text{signal},2}(t) = f\left[I_{\text{signal},1}(t), I_{\text{pump}}(t)\right]. \quad (1)$$

The function f depends on the parametric amplifier length and nonlinear coefficient.

Figure 111.2 displays two examples of behavior of the function f for a given input signal intensity, namely the relation between the output signal intensity and the pump intensity. In Fig. 111.2(a), the amplifier is unsaturated, and there is a linear relation between variations of the pump intensity and variations of the amplified signal intensity around point A. In Fig. 111.2(b), the amplifier is saturated. The output signal intensity reaches a local maximum, and there is a quadratic relation between variations of the pump intensity and variations of the amplified signal intensity around point B. Assuming that the intensity modulation of the pump does not significantly modify the instantaneous frequency of the chirped signal, the intensity of a spectral component of the amplified signal at the optical frequency ω is

$$f\left[I_{\text{signal},1}(\varphi\omega), I_{\text{pump}}(\varphi\omega)\right] = f\left[\tilde{I}_{\text{signal},0}(\omega)/\varphi, I_{\text{pump}}(\varphi\omega)\right].$$

The pump-intensity noise $\delta I_{\text{pump}}(t)$ is introduced by writing the intensity as $I_{\text{pump}}(t) = I^{(0)}_{\text{pump}}(t) + \delta I_{\text{pump}}(t)$. Assuming the amplifier is not saturated [Fig. 111.2(a)], the function f is developed to first order around the operating point set by $I^{(0)}_{\text{pump}}$ as

$$\begin{aligned} & f\left[\tilde{I}_{\text{signal},0}(\omega)/\varphi, I_{\text{pump}}(\varphi\omega)\right] \\ & = f\left[\tilde{I}_{\text{signal},0}(\omega)/\varphi, I^{0}_{\text{pump}}(\varphi\omega)\right] \\ & + \delta I_{\text{pump}}(\varphi\omega)\frac{\partial f}{\partial I_{\text{pump}}}\left[\tilde{I}_{\text{signal},0}(\omega)/\varphi, I^{0}_{\text{pump}}(\varphi\omega)\right]. \quad (2) \end{aligned}$$

The spectral intensity of the amplified recompressed signal is

$$\tilde{I}_{\text{signal},3}(\omega) = \varphi f\left[\tilde{I}_{\text{signal},0}(\omega)/\varphi, I_{\text{pump}}(\varphi\omega)\right].$$

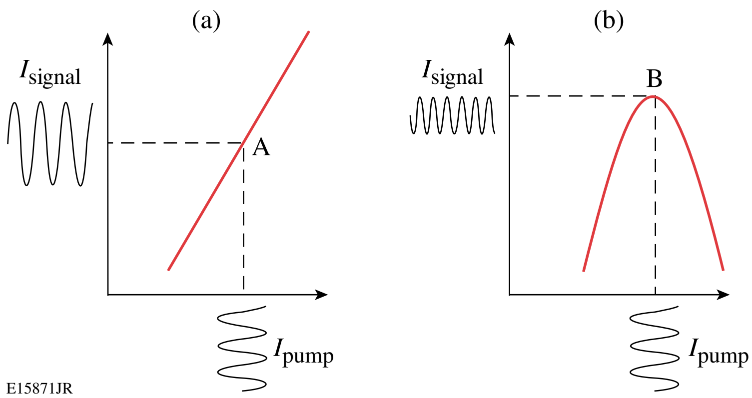

Figure 111.2
Representation of the transfer function between output signal intensity and pump intensity around the operating point of a parametric amplifier in the (a) unsaturated and (b) saturated regimes. At point A, there is a linear relation between pump-intensity modulation and amplified-signal-intensity modulation. At point B, there is a quadratic relation between pump-intensity modulation and amplified-signal-intensity modulation.

and one can define

$$\tilde{I}^{(0)}_{\text{signal},3}(\omega) = \varphi f\left[\tilde{I}_{\text{signal},0}(\omega)\big/\varphi, I^{0}_{\text{pump}}(\varphi\omega)\right]$$

as the spectral intensity of the signal amplified by a noiseless pump. The partial derivative of f with respect to the pump intensity is assumed to be independent of the signal intensity, and one defines the constant

$$f_{(1)} = \frac{\partial f}{\partial I_{\text{pump}}}\left[\tilde{I}_{\text{signal},0}(\omega)\big/\varphi, I^{0}_{\text{pump}}(\varphi\omega)\right].$$

For a compressor matched to the stretcher up to a residual spectral phase $\varphi_{\text{residual}}(\omega)$, the electric field of the recompressed signal is simply

$$\tilde{E}_{\text{signal},3}(\omega) = \sqrt{\tilde{I}^{(0)}_{\text{signal},3}(\omega) + \varphi f_{(1)}\delta I_{\text{pump}}(\varphi\omega)} \times \exp\left[i\varphi_{\text{residual}}(\omega)\right]. \tag{3}$$

A first-order development of Eq. (3) gives a spectral representation of the signal:

$$\tilde{E}_{\text{signal},3}(\omega) = \sqrt{\tilde{I}^{(0)}_{\text{signal},3}(\omega)}\exp\left[i\varphi_{\text{residual}}(\omega)\right] \times \left[1 + \frac{\varphi f_{(1)}\delta I_{\text{pump}}(\varphi\omega)}{2\tilde{I}^{(0)}_{\text{signal},3}(\omega)}\right]. \tag{4}$$

One can define

$$\tilde{E}^{(0)}_{\text{signal},3}(\omega) = \sqrt{\tilde{I}^{(0)}_{\text{signal},3}(\omega)}\exp\left[i\varphi_{\text{residual}}(\omega)\right]$$

as the electric field of the recompressed signal in the absence of noise. In the OPCPA process, the spectral density of the amplified signal is usually approximately constant (or slowly varying) because of saturation effects, so that $\tilde{I}^{(0)}_{\text{signal},3}(\omega)$ is replaced by $\varphi I_{\text{signal},2}$ in the denominator of Eq. (4). This leads to

$$\tilde{E}_{\text{signal},3}(\omega) = \tilde{E}^{(0)}_{\text{signal},3}(\omega)\left[1 + \frac{f_{(1)}\delta I_{\text{pump}}(\varphi\omega)}{2I_{\text{signal},2}}\right]. \tag{5}$$

The Fourier transform of Eq. (5) gives the electric field in the temporal domain:

$$E_{\text{signal},3}(t) = E^{(0)}_{\text{signal},3}(t) + \frac{f_{(1)}}{2I_{\text{signal},2}\varphi} \times E^{(0)}_{\text{signal},3}(t) \otimes \delta\tilde{I}_{\text{pump}}(t/\varphi). \tag{6}$$

Further simplification stems from defining

$$f_{(1,N)} = f_{(1)} I^{(0)}_{\text{pump}}\big/I_{\text{signal},2},$$

which is the change in intensity of the amplified signal normalized to the intensity of the amplified signal for a change in the pump intensity normalized to the pump intensity. The field of the recompressed signal is

$$E_{\text{signal},3}(t) = E^{(0)}_{\text{signal},3}(t) + \frac{f_{(1,N)}}{2\varphi I^{(0)}_{\text{pump}}} \times E^{(0)}_{\text{signal},3}(t) \otimes \delta\tilde{I}_{\text{pump}}(t/\varphi), \tag{7}$$

and the intensity of the compressed signal is

$$I_{\text{signal},3}(t) = I^{(0)}_{\text{signal},3}(t) + \frac{f^2_{(1,N)}}{4\left[\varphi I^{(0)}_{\text{pump}}\right]^2} \times \left| E^{(0)}_{\text{signal},3}(t) \otimes \delta\tilde{I}_{\text{pump}}(t/\varphi)\right|^2, \tag{8}$$

using the fact that the first term in the right-hand side of Eq. (7) is a short pulse while the second term describes the contrast reduction over a large temporal range.

When the amplifier is saturated [Fig. 111.2(b)], $f_{(1)} = 0$ and Eq. (2) must be replaced by the second-order decomposition of f, which is

$$\begin{aligned} f\left[\tilde{I}_{\text{signal},0}(\omega)/\varphi, I_{\text{pump}}(\varphi\omega)\right] &= f\left[\tilde{I}_{\text{signal},0}(\omega)/\varphi, I^{(0)}_{\text{pump}}(\varphi\omega)\right] \\ &+ \frac{1}{2}\left[\delta I_{\text{pump}}(\varphi\omega)\right]^2 \\ &\times \frac{\partial^2 f}{\partial I^2_{\text{pump}}}\left[\tilde{I}_{\text{signal},0}(\omega)/\varphi, I^{(0)}_{\text{pump}}(\varphi\omega)\right]. \end{aligned} \tag{9}$$

Assuming that the second-order derivative of f with respect to the pump intensity does not depend on the signal intensity, one defines

$$f_{(2)} = \partial^2 f \Big/ \partial I^2_{\text{pump}}\left[\tilde{I}_{\text{signal},0}(\omega)/\varphi, I^{(0)}_{\text{pump}}(\varphi\omega)\right].$$

Replacing $\tilde{I}^{(0)}_{\text{signal},3}(\omega)$ by $\varphi I_{\text{signal},2}$, one obtains

$$\tilde{E}_{\text{signal},3}(\omega) = \tilde{E}^{(0)}_{\text{signal},3}(\omega)\left[1 + \frac{f_{(2)}\delta I^2_{\text{pump}}(\varphi\omega)}{4I_{\text{signal},2}}\right]. \tag{10}$$

The Fourier transform of Eq. (10) gives the temporal field of the recompressed signal:

$$E_{\text{signal},3}(t) = E^{(0)}_{\text{signal},3}(t) + \frac{f_{(2,N)}}{4\left[\varphi I^{(0)}_{\text{pump}}\right]^2} E^{(0)}_{\text{signal},3}(t) \otimes \delta\tilde{I}_{\text{pump}}(t/\varphi) \otimes \delta\tilde{I}_{\text{pump}}(t/\varphi), \tag{11}$$

where $f_{(2,N)} = f_{(2)}\left[I^{(0)}_{\text{pump}}\right]^2 \Big/ I_{\text{signal},2}$ is the normalized change in the amplified signal intensity for a normalized change in the pump intensity. Finally, the intensity of the recompressed signal is

$$I_{\text{signal},3}(t) = I^{(0)}_{\text{signal},3}(t) + \frac{f^2_{(2,N)}}{16\left[\varphi I^{(0)}_{\text{pump}}\right]^4} \times \left| E_{\text{signal},3}(t) \otimes \delta\tilde{I}_{\text{pump}}(t/\varphi) \otimes \delta\tilde{I}_{\text{pump}}(t/\varphi)\right|^2. \tag{12}$$

Equations (8) and (12) are general expressions linking the variations in pump intensity to the intensity of the recompressed pulse in the two practically relevant cases: $f_{(1)} \neq 0$ describes the linear modulation regime, with a linear relation between the pump intensity and the amplified stretched signal intensity around the operating point; $f_{(1)} = 0, f_{(2)} \neq 0$ describe the quadratic modulation regime, with a quadratic relation between the pump intensity and the amplified stretched signal intensity around the operating point. In the next two subsections these general expressions are evaluated when ASE is present on the pump pulse.

3. Contrast Degradation of an OPCPA System in the Linear-Modulation Regime due to the Pump-Pulse ASE

The pump-pulse ASE is described as an additive stationary process E_{ASE}, and the field of the pump pulse is

$$E_{\text{pump}}(t) = E^{(0)}_{\text{pump}}(t) + E_{\text{ASE}}(t). \tag{13}$$

One has at first order

$$I_{\text{pump}}(t) = I_{\text{pump}}^{(0)}(t) + E_{\text{pump}}^{(0)}(t) E_{\text{ASE}}^{*}(t) + E_{\text{pump}}^{(0)*}(t) E_{\text{ASE}}(t),$$

which allows one to identify

$$\delta I_{\text{pump}}(t) = E_{\text{pump}}^{(0)}(t) E_{\text{ASE}}^{*}(t) + E_{\text{pump}}^{(0)*}(t) E_{\text{ASE}}(t).$$

One can use the simplification

$$E_{\text{pump}}^{(0)}(t) = E_{\text{pump}}^{(0)*}(t) = \sqrt{I_{\text{pump}}^{(0)}}$$

over the interval $[0,T]$, where the pump has significant intensity, and set the ASE electric field to 0 outside the interval $[0,T]$. The electric field of one realization of the ASE restricted to the interval $[0,T]$ and its Fourier transform are noted $E_{\text{ASE},T}$ and $\tilde{E}_{\text{ASE},T}$, respectively. One obtains

$$\delta \tilde{I}_{\text{pump}}(\omega) = \sqrt{I_{\text{pump}}^{(0)}} \left[\tilde{E}_{\text{ASE},T}(\omega) + \tilde{E}_{\text{ASE},T}^{*}(-\omega)\right]. \quad (14)$$

In the linear modulation regime, the calculation of the intensity of the recompressed pulse using this expression and Eq. (8) leads to

$$I_{\text{signal},3}(t) = I_{\text{signal},3}^{(0)}(t) + \frac{f_{(1,N)}^{2}}{4\varepsilon_{\text{pump}}} \int I_{\text{signal},3}^{(0)}(t - \varphi\omega') \times \left[\tilde{I}_{\text{ASE},T}(\omega') + \tilde{I}_{\text{ASE},T}(-\omega')\right] d\omega', \quad (15)$$

where $\varepsilon_{\text{pump}}$ is the energy of the pump pulse. The pump-induced pedestal is therefore given by a convolution of the symmetrized spectrum of the ASE present on the pump pulse with the recompressed pulse intensity. The intensity of the pedestal is proportional to $f_{(1,N)}^{2}$. Proper spectral filtering of the pump pulse reduces the temporal extent of the induced pedestal. In the usual case where the recompressed pulse is significantly shorter than the temporal variations of the induced pedestal, Eq. (15) can be simplified as

$$I_{\text{signal},3}(t) = I_{\text{signal},3}^{(0)}(t) + \frac{f_{(1,N)}^{2} \varepsilon_{\text{signal}}^{(0)}}{4\varphi\varepsilon_{\text{pump}}} \times \left[\tilde{I}_{\text{ASE},T}(t/\varphi) + \tilde{I}_{\text{ASE},T}(-t/\varphi)\right]. \quad (16)$$

The pedestal due to the ASE present on the pump pulse is therefore directly given by a symmetrized version of the spectrum of the ASE present on the pump pulse. The symmetrized spectrum of the ASE is spread in time proportionally to the second-order dispersion of the chirped pulse. Integration of Eq. (15) gives

$$\varepsilon_{\text{signal}} = \varepsilon_{\text{signal}}^{(0)} \left[1 + f_{(1,N)}^{2} \varepsilon_{\text{ASE},T} / 2\varepsilon_{\text{pump}}\right],$$

which allows the energy in the pedestal $\varepsilon_{\text{pedestal}}$ normalized to the energy of the signal $\varepsilon_{\text{signal}}^{(0)}$ to be expressed as

$$\frac{\varepsilon_{\text{pedestal}}}{\varepsilon_{\text{signal}}^{(0)}} = \frac{f_{(1,N)}^{2}}{2} \frac{\varepsilon_{\text{ASE},T}}{\varepsilon_{\text{pump}}}. \quad (17)$$

The ratio of the pedestal energy to the signal energy,

$$\varepsilon_{\text{pedestal}} / \varepsilon_{\text{signal}}^{(0)},$$

is directly proportional to the ratio of the energy of the ASE in the temporal range defined by the pump to the energy of the pump. The ratio $\varepsilon_{\text{ASE},T}/\varepsilon_{\text{pump}}$ is called "fractional ASE energy" in the remainder of this article.

4. Contrast Degradation of an OPCPA System in the Quadratic-Modulation Regime due to the Pump ASE

The intensity of the recompressed pulse for an OPCPA system in the quadratic-modulation regime with ASE present on the pump can be calculated using Eqs. (12) and (14):

$$I_{\text{signal},3}(t) = I_{\text{signal},3}^{(0)}(t) + \frac{f_{(2,N)}^{2}}{8\left(\varphi\varepsilon_{\text{pump}}\right)^{2}} I_{\text{signal},3}^{(0)}(t) \otimes \left[\tilde{I}_{\text{ASE},T}(t/\varphi) + \tilde{I}_{\text{ASE},T}(-t/\varphi)\right] \otimes \left[\tilde{I}_{\text{ASE},T}(t/\varphi) + \tilde{I}_{\text{ASE},T}(-t/\varphi)\right]. \quad (18)$$

Equation (18) shows that the pedestal is given by the double convolution of the symmetrized spectrum of the pump ASE with the recompressed signal in the absence of pump ASE. The convolution of the symmetrized spectrum of ASE with itself is broader than the spectrum of ASE (e.g., by a factor $\sqrt{2}$ for a Gaussian spectrum). Therefore, the temporal extent of the pedestal is larger than in the linear-modulation regime. In the case where the intensity of the recompressed signal is short compared to the temporal variations of the pedestal, Eq. (18) can be simplified into

$$I_{\text{signal},3}(t) = I^{(0)}_{\text{signal},3}(t) + \frac{f^2_{(2,N)}\varepsilon^{(0)}_{\text{signal}}}{8\varphi^2\varepsilon^2_{\text{pump}}} \times \left[\tilde{I}_{\text{ASE},T}(t/\varphi) + \tilde{I}_{\text{ASE},T}(-t/\varphi)\right] \otimes \left[\tilde{I}_{\text{ASE},T}(t/\varphi) + \tilde{I}_{\text{ASE},T}(-t/\varphi)\right]. \tag{19}$$

Finally, integrating Eq. (18) leads to the energy in the pedestal,

$$\frac{\varepsilon_{\text{pedestal}}}{\varepsilon^{(0)}_{\text{signal}}} = \frac{f^2_{(2,N)}\varepsilon^2_{\text{ASE},T}}{2\varepsilon^2_{\text{pump}}}. \tag{20}$$

In the quadratic-modulation regime, the ratio of the energy of the pedestal to the energy of the signal is proportional to the square of the fractional ASE energy. Comparing Eq. (20) with Eq. (17) leads to the conclusion that if $\varepsilon_{\text{ASE},T}/\varepsilon_{\text{pump}} < \left[f_{(1,N)}/f_{(2,N)}\right]^2$, there is less energy in the pedestal when the amplifier is run in the quadratic-modulation regime. Operating the OPCPA in the saturation regime locally decreases the modulation of the output intensity and reduces the total energy of the associated temporal pedestal, provided that the previous inequality is verified.

Simulations of Pump-Induced Contrast Degradation

1. Model Description

Simulations of an OPCPA system with parameters similar to those of the OPCPA preamplifier of LLE's Multi-Terawatt laser[10] and the front end of the OMEGA EP Laser Facility[17] have been performed. The signal has a central wavelength equal to 1053 nm. The case of a flat spectral density has been simulated since it corresponds closely to the derivations performed in the previous section. The case of a Gaussian spectral density with a full width at half maximum (FWHM) equal to 6 nm has also been simulated since it is closer to the actual experimental conditions. The stretcher introduces a dispersion equal to 300 ps/nm, i.e., $\varphi = 1.76 \times 10^{22}$ s^2. The preamplifier has two lithium triborate (LBO) crystals cut for type-I phase matching at 1053 nm and 526.5 nm in collinear interaction, i.e., $\varphi_{\text{LBO}} = 11.8°$ and $\theta_{\text{LBO}} = 90°$, with a total length of 59.5 mm. The OPCPA pump at 526.5 nm is obtained by doubling a pump pulse at 1053 nm in an 11-mm LBO crystal. The pump at 1053 nm is a 20th-order super-Gaussian, with a FWHM equal to 2.6 ns. The intensity of the up-converted pump has been obtained using a Runge–Kutta resolution of the corresponding nonlinear equations. Figure 111.3 displays the normalized intensity of the pump and stretched signal in the OPCPA crystal. The operation of the preamplifier was simulated by solving the system of three equations describing the parametric interaction of the electric field of the signal, idler, and pump using the Runge–Kutta method. No spatial resolution or temporal effects have been introduced, for the reasons expressed at the beginning of the previous section. It is straightforward (although computationally more intensive) to introduce these effects. The phase mismatch between the interacting waves was chosen equal to zero. Figure 111.4 displays the amplified stretched signal intensity as a function of the pump intensity for an input stretched signal intensity of 0.1 W/cm^2, i.e., the function $I_{\text{signal},2} = f\left[I_{\text{signal},1}, I_{\text{pump}}\right]$ used in the previous section for $I_{\text{signal},1} = 0.1$ W/cm^2. Points A and B correspond to the linear- and quadratic-modulation regimes, respectively. A fit of the curve plotted in Fig. 111.4 around these two points leads to the values $f_{(1,N)} = 8$ and $f_{(2,N)} = 66$. The next two subsections present the contrast degradation results for a pump with ASE and a signal with constant spectral density followed by results for a pump with ASE and a signal with a Gaussian spectral density. For the sake of clarity, the intensity of the recompressed signal is plotted only at negative times (i.e., before the peak of the signal), bearing in mind that the pump-induced contrast degradation is symmetric.

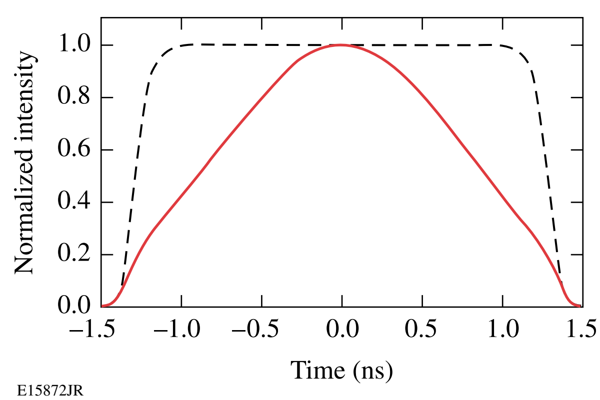

Figure 111.3
Normalized intensity of the chirped Gaussian signal (solid curve) and pump (dashed curve) in the OPCPA system.

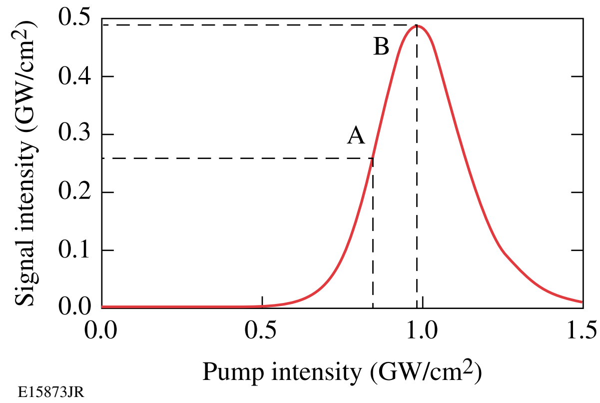

Figure 111.4
Transfer function of the OPCPA preamplifier for a signal intensity equal to 0.1 W/cm^2. Points A and B identify the linear and quadratic regimes of operation, respectively.

2. Pump with ASE and Signal with Flat Spectral Density

In this section, the stretched signal has a flat spectral density and an intensity of 0.1 W/cm^2. The pump ASE spectrum is assumed Gaussian and centered at the wavelength of the pump pulse. The FWHM of the spectrum is chosen equal to either 0.14 nm (which was experimentally measured on the Nd:YLF regenerative amplifier used to generate the pump pulse) or 0.03 nm (which corresponds to a hypothetical pump spectral bandpass filtering). Figure 111.5 displays close-ups of the simulated intensity of the pump for an ASE bandwidth of 0.14 nm and 0.03 nm at various fractional ASE energies $\varepsilon_{\mathrm{ASE},T}/\varepsilon_{\mathrm{pump}}$. The homodyne beating of the electric field of the ASE with the electric field of the pump leads to significant pump intensity modulation even at low ASE energy levels. Figure 111.6 displays a comparison of the results of the simulation with the analytical results for the 0.14-nm bandwidth. The OPCPA is run either in the linear modulation regime [Figs. 111.6(a)–111.6(c)] or in the quadratic-modulation regime [Figs. 111.6(d)–111.6(f)]. The fractional ASE energy is specified as 10^{-5}, 10^{-4}, and 10^{-3}. Significant pedestal levels are observed, even for relatively low pump intensity modulation, indicating that such contrast degradation can severely limit OPCPA systems, or laser systems that include an OPCPA as one of their amplifiers. Good agreement of the simulations with the analytical predictions is obtained. Discrepancy in the quadratic modulation regime at low fractional ASE energies is attributed to the leading and the falling edge of the pump, for which the amplification process is in the linear regime. The pedestal due to the pump ASE extends at longer times in the case of quadratic modulation, as expected from the double convolution of Eq. (18). The pedestal is typically more intense at short times in the linear regime, and it can also be seen that the total energy in the

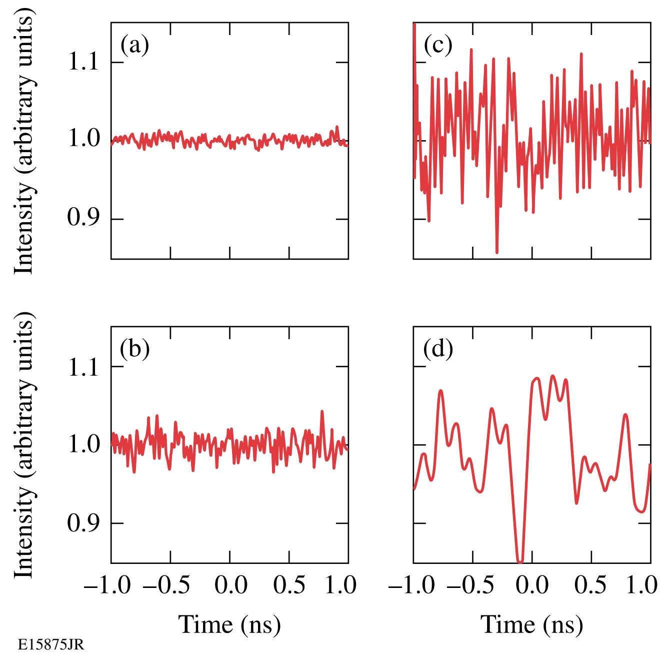

Figure 111.5
Close-ups of the temporal intensity of the pump for ASE with a Gaussian spectrum with a FWHM equal to 0.14 nm and a fractional energy equal to (a) 10^{-5}, (b) 10^{-4}, and (c) 10^{-3}, and (d) for ASE with a Gaussian spectrum with a FWHM equal to 0.03 nm and a fractional energy equal to 10^{-3}.

pedestal is smaller in the quadratic modulation regime than in the linear modulation regime {in agreement with the relation $\varepsilon_{\mathrm{ASE},T}/\varepsilon_{\mathrm{pump}} < \left[f_{(1,N)}/f_{(2,N)}\right]^2$, with $\left[f_{(1,N)}/f_{(2,N)}\right]^2 = 0.014$}. It should be noted, however, that the two modulation regimes lead to similar pedestal levels around –100 ps. Figures 111.7(a) and 111.7(d) display the intensity of the recompressed signal for an ASE bandwidth of 0.03 nm and a fractional ASE energy equal to 10^{-3}, which can be compared to the intensity plotted in Figs. 111.6(c) and 111.6(f). Reduction of the bandwidth of the pump ASE leads to a drastic improvement of the signal temporal contrast. This result shows that a significant increase in the contrast of OPCPA systems can be obtained via proper spectral filtering of the pump pulse, as is discussed in **Experimental Demonstration of Temporal Contrast Improvement of an OPCPA System by Pump Spectral Filtering** (p. 144). While this was expressed previously in terms of the coherence time of the pump ASE,[19] the temporal contrast away from the peak of the signal is influenced mostly by the spectral density of the ASE at optical frequencies significantly different from the central frequency of the pump. A non-zero spectral density at these optical frequencies leads to a finite extinction ratio for the pulse. The coherence time of the ASE describes the variations of the temporal electric field of the ASE due to interference between different optical frequencies in the ASE spectrum.

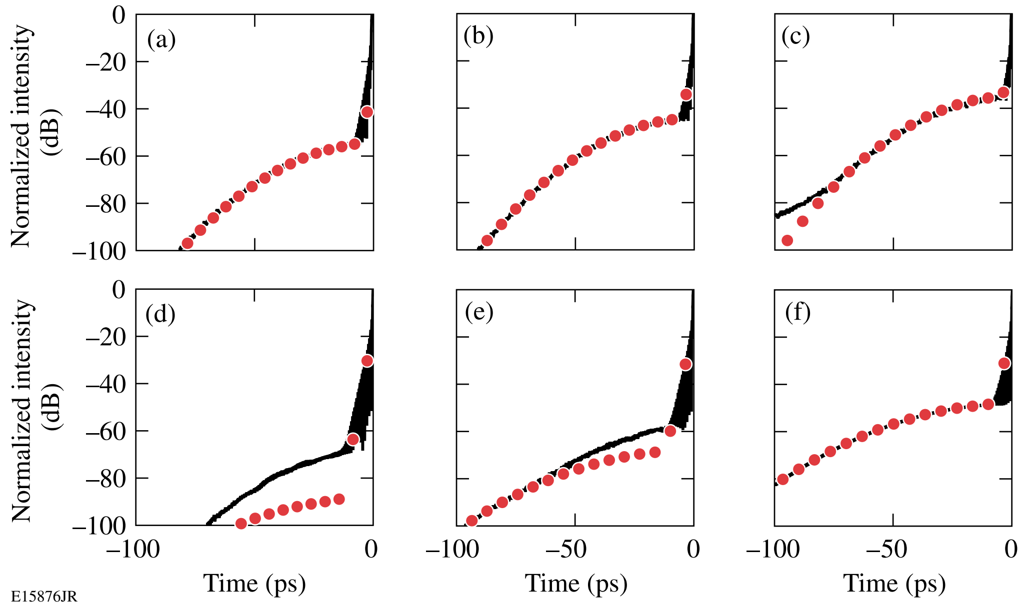

Figure 111.6
Intensity of the recompressed signal for an input signal with a flat spectral density and an ASE Gaussian spectrum with a FWHM equal to 0.14 nm. (a)–(c) correspond to an amplifier run in the linear-modulation regime when the fractional ASE energy is equal to (a) 10^{-5}, (b) 10^{-4}, and (c) 10^{-3}. (d)–(f) correspond to an amplifier run in the quadratic-modulation regime when the fractional ASE energy is equal to (d) 10^{-5}, (e) 10^{-4}, and (f) 10^{-3}. In each case, the simulated intensity is plotted with a continuous line, and the intensity predicted analytically is plotted with solid circles.

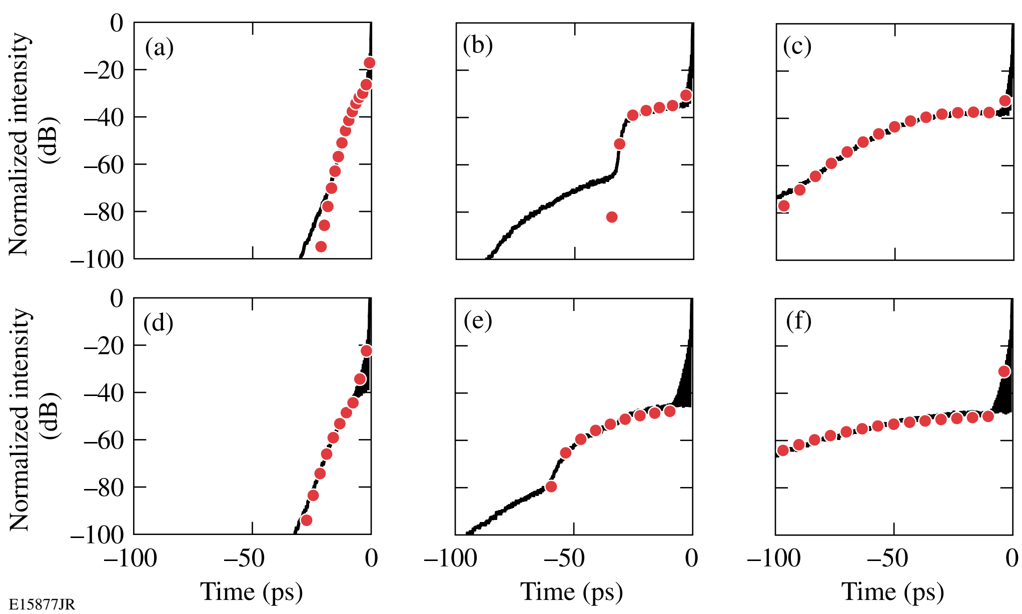

Figure 111.7
Intensity of the recompressed signal for an input signal with a flat spectral density, ASE with various Gaussian spectra, and fractional ASE energy equal to 10^{-3}. (a) and (d) correspond to a FWHM equal to 0.03 nm in the linear and quadratic modulation regimes, respectively. (b) and (e) correspond to a FWHM equal to 0.14 nm filtered by a 0.20-nm FWHM, 20th-order super-Gaussian filter in the linear and quadratic modulation regimes, respectively. (c) and (f) correspond to a FWHM equal to 0.14 nm centered 0.07 nm away from the central wavelength of the pump in the linear and quadratic modulation regimes. In each case, the simulated intensity is plotted with a continuous line, and the intensity predicted analytically is plotted with solid circles.

However, the modulations of pump intensity are mostly due to the interference between optical frequencies of the noiseless pump pulse and optical frequencies of the pump ASE. Figure 111.7 presents simulations and analytic predictions for two different ASE spectra that have a FWHM equal to 0.14 nm, i.e., the same coherence time, for a fractional ASE energy equal to 10^{-3}. In the first case [Figs. 111.7(b) and 111.7(e)], a 20th-order super-Gaussian filter with 0.20-nm FWHM has been used to filter the ASE. A large decrease in the level of the pedestal is observed away from the peak of the pulse, although the pedestal conserved its value closer to the peak, as expected from the dependence of the pedestal to the spectrum of the ASE. In the second case [Figs. 111.7(c) and 111.7(f)], the ASE has a Gaussian spectrum with 0.14-nm FWHM centered 0.07 nm away from the central wavelength of the pump. The contrast is significantly degraded compared to Figs. 111.6(c) and 111.6(f), and an increase of the pedestal intensity by approximately 20 dB is observed. Optimization of the contrast can be performed by proper spectral filtering of the pump. A narrow filter on the pump pulse increases the contrast of the recompressed signal and is not detrimental to the operation of the OPCPA system as long as the pump pulse is not temporally distorted by the spectral filter. Generally speaking, the pedestal shape, extent, and intensity vary significantly with the energy of the ASE, its spectrum, and the regime of operation of the amplifier.

3. Pump with ASE and Signal with Gaussian Spectral Density

In this section, the spectral density of the signal is assumed Gaussian, and the intensity of the stretched signal varies significantly as a function of time, taking its maximal value of 0.1 W/cm^2 at the peak of the pulse. The condition that the first-order derivative or second-order derivative of the function *f* as a function of the intensity of the signal is independent of the signal intensity is not strictly verified. Some temporal components (i.e., spectral components) of the signal have an optical intensity placing them in the quadratic-modulation regime for the OPCPA process, but other components have an optical intensity placing them in the linear-modulation regime. The contrast of the recompressed signal is generally linked in a nontrivial manner to the noise of the pump pulse. Figure 111.8 displays the transfer function between pump intensity and output signal intensity for a signal input intensity equal to 0.1 W/cm^2 and 0.05 W/cm^2. While the pump intensity corresponding to point B ensures that the output signal intensity is approximately the same for these two input signal intensities (i.e., the spectral density of the amplified pulse does not depend on the wavelength at first order), it allows operation only in the quadratic-modulation regime for the highest signal intensity. Figure 111.9 presents the intensities simulated with ASE parameters identical to those of Fig. 111.6. The analytical results plotted on this figure correspond to the stretched signal pulse with a constant intensity of 0.1 W/cm^2. For the linear- and quadratic-modulation regimes, no significant difference between the two sets of simulations is observed, and the analytical derivation is still in good agreement with the simulations. In the linear regime for the peak intensity of the stretched pulse, all of the optical frequencies in the pulse are in a similar linear regime, and the resulting contrast is equivalent to the contrast obtained for a constant spectral density. The discrepancy observed for low ASE energy in the quadratic regime is more prevalent in this case, which indicates that additional contribution to the

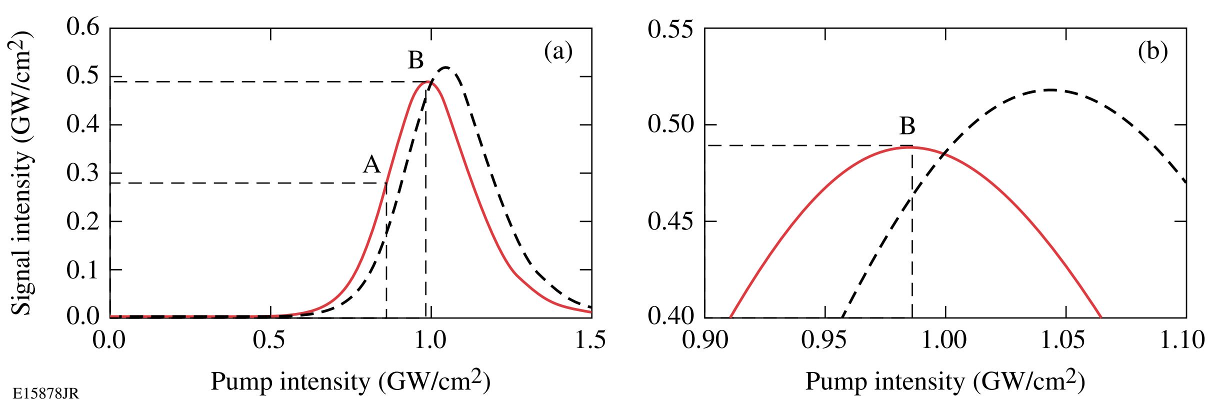

Figure 111.8
Transfer function of the parametric preamplifier for a signal intensity equal to 0.1 W/cm^2 (solid curve) and 0.05 W/cm^2 (dashed curve). Points A and B represent the linear- and quadratic-modulation regimes for the OPCPA system for a stretched signal intensity of 0.1 W/cm^2. (a) Full transfer function; (b) close-up around point B.

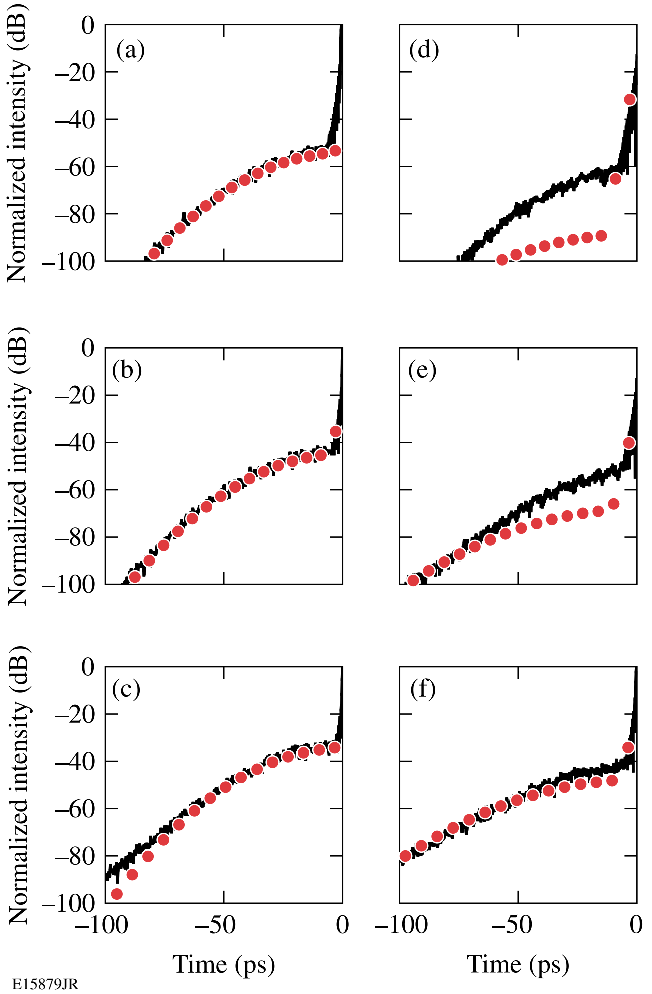

Figure 111.9
Intensity of the recompressed signal for an input signal with a Gaussian spectral density and ASE with a Gaussian spectrum with a FWHM equal to 0.14 nm. (a)–(c) correspond to an amplifier run in the linear-modulation regime when the fractional ASE energy is equal to (a) 10^{-5}, (b) 10^{-4}, and (c) 10^{-3}. (d)–(f) correspond to an amplifier run in the quadratic-modulation regime when the fractional ASE energy is equal to (d) 10^{-5}, (e) 10^{-4}, and (f) 10^{-3}. In each case, the simulated intensity is plotted with a continuous line, and the intensity predicted analytically is plotted with solid circles.

pedestal is present due to some components of the signal in the linear-modulation regime. The coupling between pump intensity and amplified signal intensity for these wavelengths is smaller than at point A of Fig. 111.4. A fit of the dashed curve of Fig. 111.8 at its intersection with the vertical dashed line representing the pump intensity for these simulations leads to $f_{(1,N)} = 4$, which implies a smaller impact of the pump intensity modulation. These results demonstrate that, in the general case, both linear- and quadratic-modulation regimes influence the induced pedestal on an OPCPA system.

Experimental Demonstration of Temporal Contrast Improvement of an OPCPA System by Pump Spectral Filtering

1. Experimental Setup

A general approach to significantly improve the contrast of OPCPA systems by spectrally filtering the pump pulse has been experimentally demonstrated. Simple and efficient filtering of the pump pulse is performed in a regenerative amplifier using a VBG, and the bandwidth of the filtering is narrowed significantly by the large number of round-trips in the cavity. Contrast improvement by regenerative spectral filtering was performed on the prototype front end of the OMEGA EP Laser Facility (Fig. 111.10).[10,17] The pump pulse is generated by a fiber integrated front-end source (IFES), where a 2.4-ns pulse around 1053 nm is temporally shaped to precompensate the square-pulse distortion during amplification. This pulse is amplified at 5 Hz from 100 pJ to 4 mJ in a diode-pumped regenerative amplifier (DPRA).[20] One of the flat end-cavity mirrors of the DPRA is replaced by the VBG and a flat mirror, so that the mirror acts as the DPRA end-cavity mirror and the beam is reflected twice per round-trip on the VBG. The incidence angle on the VBG, designed for high reflection at 1057.5 nm at normal incidence, is approximately 7° to provide maximum reflection at 1053 nm. The VBG is a bulk piece of photothermorefractive glass, where a grating is permanently written by UV illumination followed by thermal development.[21] The damage threshold of similar VBG's has been found to be higher than 10 J/cm^2 in the nanosecond regime. With sol-gel antireflection coating, the VBG has a single-pass reflectivity of 99.4% at 1053 nm, and the slight increase in the DPRA build-up time due to the additional losses was compensated by increasing the diode-pump current. No change in the output beam spatial profile was observed. Without active temperature control of the VBG, the DPRA operated for several days in a temperature-controlled room with no variation in performance. (Additional characterization can be found in Ref. 22.) The bandwidth of the VBG reflectivity around 1057.5 nm is 230 pm, which, assuming a Gaussian shape, should provide a 23-pm bandwidth after 50 round-trips in the DPRA, with two reflections on the VBG per round-trip. With the intracavity VBG, the unseeded DPRA output spectrum shows a reduction of the bandwidth of the DPRA from 146 pm to 41 pm, but is broad enough to amplify the pump pulse without distortion (Fig. 111.11). Subsequent amplification to 2 J is performed by four passes in a crystal large-aperture ring amplifier containing two flash-lamp–pumped Nd:YLF rods, after apodization of the DPRA beam.[23] Frequency conversion to 526.5 nm occurs in an 11-mm LBO crystal with an efficiency of 70%. Filtering in the DPRA decreases the amount of ASE from the IFES and

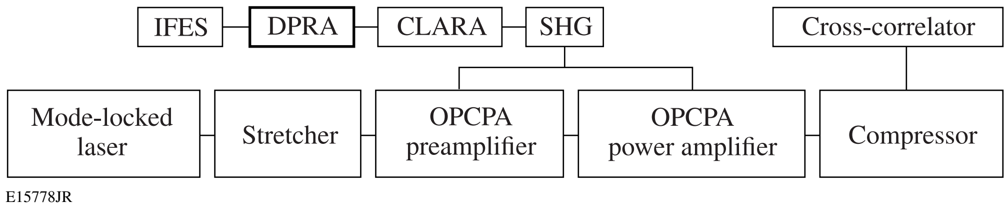

Figure 111.10
Schematic of the laser system. IFES: integrated front-end source; DPRA: diode-pumped regenerative amplifier; CLARA: crystal large-aperture ring amplifier; SHG: sum-harmonic generation. Filtering of the pump pulse is performed in the DPRA (shown above in bold).

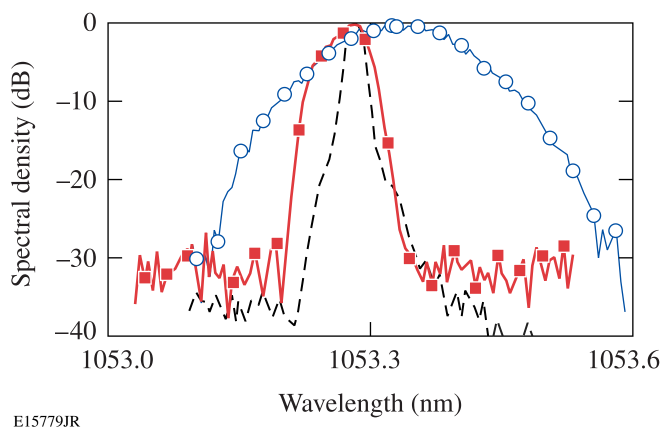

Figure 111.11
Optical spectrum of the unseeded DPRA measured with a mirror in the cavity (thin solid curve with open circles) and with the VBG in the cavity (solid curve with solid squares). The optical spectrum of the signal amplified by the DPRA (dashed curve) is limited by the resolution of the optical spectrum analyzer and is significantly narrower than the unseeded DPRA with the intracavity VBG.

from the DPRA itself (these two high-gain stages having the largest contribution to the pump ASE) and benefits from the large number of reflections on the filter.

The OPCPA system is composed of a mode-locked laser operating at 1053 nm, an Öffner-triplet stretcher providing a dispersion of 300 ps/nm, a preamplifier with two 29.75-mm LBO crystals in a walk-off compensating geometry, a power amplifier with one 16.5-mm LBO crystal, and a two-grating compressor in a double-pass configuration. The pump pulse is split to pump the preamplifier and power amplifier. Amplification of the signal to 250 mJ is achieved, and a portion of the amplified pulse is sent to the diagnostic compressor.

2. Experimental Results

The temporal contrast was measured using a scanning third-order cross-correlator (Sequoia, Amplitude Technologies). The dynamic range of the diagnostics is 10^{11} but is limited to 10^{8} by the parametric fluorescence from the OPCPA system. Postpulses are due to multiple reflections in the cross-correlator and are of no practical concern. Figure 111.12 displays the cross-correlations measured (a) when the preamplifier and power amplifier are operated at full energy, (b) when only the preamplifier is operated at saturation, and (c) when only the preamplifier is operated at half its nominal output power. The prepulse contrast is consistently improved with the intracavity VBG. The pump-induced contrast degradation is particularly important in the preamplifier, even when it is run at saturation, and a contrast improvement of the order of 20 dB is observed. When the preamplifier is run at half output power, a larger coupling between the pump intensity and the amplified signal intensity magnifies the impact of the pump noise on the contrast. These two operating points correspond to the linear- and quadratic-modulation regimes for the preamplifier, as identified by points A and B in Fig. 111.4. The choice of the crystals and pump intensities in this system reduces the spatial-intensity modulations in the amplified signal. This decreases the temporal-intensity modulations in the amplified signal and reduces the impact of the pump-intensity variations on the contrast of the recompressed pulse. Most OPCPA systems are not designed with these considerations in mind, and the contrast improvement is expected to be significant for these systems.

The optical signal-to-noise ratio (OSNR) of the OPCPA pump pulse was reduced by decreasing the average power of the monochromatic source in the IFES from its nominal value of 10 mW to 2 mW, 0.4 mW, and 0.1 mW, and compensating the reduced output energy by increasing the DPRA diode pump current. The reduced OSNR is due to the reduced seed level in both the IFES fiber amplifier and the DPRA. Figure 111.13 displays the cross-correlations measured when the preamplifier and power amplifier are operated in nominal conditions [the cross-correlations measured for the nominal value of 10 mW can be seen in Fig. 111.12(a)]. Without spectral filtering, a large increase in the temporal pedestal is observed, and the contrast

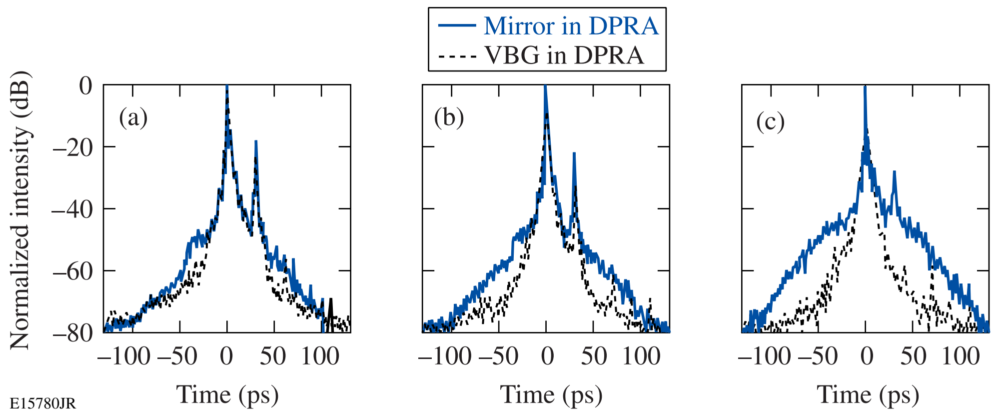

Figure 111.12
Third-order scanning cross-correlation of the OPCPA output pulse (a) when the preamplifier and power amplifier are operated at full energy, (b) when only the preamplifier is operated at saturation, and (c) when only the preamplifier is operated at half its nominal output power. In each case, the cross-correlation measured with the mirror in the DPRA is plotted with a solid line, and the cross-correlation measured with the VBG in the DPRA is plotted with a dashed line.

50 ps before the peak of the pulse is 54 dB, 46 dB, and 35 dB, respectively, for a 2-mW, 0.4-mW, and 0.1-mW average power. No contrast degradation is observed with the filtered DPRA, and the contrast 50 ps before the peak of the pulse is consistently equal to 68 dB.

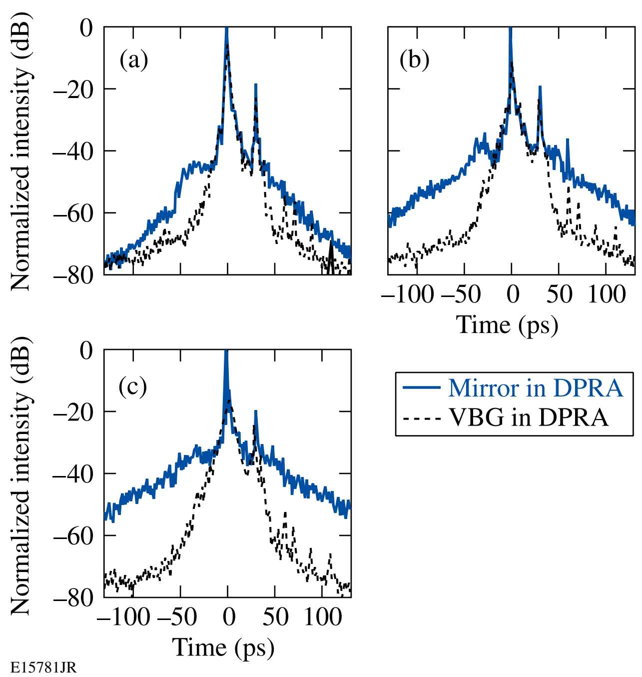

Figure 111.13
Third-order scanning cross-correlation of the OPCPA output pulse when the average power of the monochromatic laser of IFES is reduced from 10 mW to (a) 2 mW, (b) 0.4 mW, and (c) 0.1 mW. In each case, the cross-correlation measured with the mirror in the DPRA is plotted with a solid line, and the cross-correlation measured with the VBG in the DPRA is plotted with a dashed line.

Conclusions

An analysis of pump-induced contrast degradation in an OPCPA system has been performed. The general link between pump modulation and the contrast of the recompressed pulse has been derived in the two cases of practical interest, for which pump-intensity modulation couples either linearly or quadratically to the amplified signal intensity during the parametric process. Analytical expressions linking the spectrum of the ASE present on the pump pulse to the temporal pedestal of the signal amplified in the OPCPA system have been derived and compared to simulations. Significant reduction of the induced temporal pedestal was experimentally demonstrated in an OPCPA system by filtering the pump pulse during its amplification in a regenerative amplifier. The general expressions of the contrast degradation should prove useful for understanding the contrast limitation of current OPCPA systems and predicting the performance of future systems. The demonstrated solution is simple to implement and is applicable to most OPCPA systems.

ACKNOWLEDGMENT

This work was supported by the U.S. Department of Energy Office of Inertial Confinement Fusion under Cooperative Agreement No. DE-FC52-92SF19460, the University of Rochester, and the New York State Energy Research and Development Authority. The support of DOE does not constitute an endorsement by DOE of the views expressed in this article.

REFERENCES

1. D. Umstadter, Phys. Plasmas **8**, 1774 (2001).
2. S.-W. Bahk *et al.*, Opt. Lett. **29**, 2837 (2004).
3. J. D. Zuegel, S. Borneis, C. Barty, B. LeGarrec, C. Danson, N. Miyanaga, P. K. Rambo, C. LeBlanc, T. J. Kessler, A. W. Schmid,

L. J. Waxer, J. H. Kelly, B. Kruschwitz, R. Jungquist, E. Moses, J. Britten, I. Jovanovic, J. Dawson, and N. Blanchot, Fusion Sci. Technol. **49**, 453 (2006).

4. M. Nantel *et al.*, IEEE J. Sel. Top. Quantum Electron. **4**, 449 (1998).
5. V. Bagnoud, J. D. Zuegel, N. Forget, and C. Le Blanc, Opt. Express **15**, 5504 (2007).
6. A. Dubietis, G. Jonusauskas, and A. Piskarskas, Opt. Commun. **88**, 437 (1992).
7. I. N. Ross *et al.*, Opt. Commun. **144**, 125 (1997).
8. A. Dubietis, R. Butkus, and A. P. Piskarskas, IEEE J. Sel. Top. Quantum Electron. **12**, 163 (2006).
9. H. Yoshida *et al.*, Opt. Lett. **28**, 257 (2003).
10. V. Bagnoud, I. A. Begishev, M. J. Guardalben, J. Puth, and J. D. Zuegel, Opt. Lett. **30**, 1843 (2005).
11. N. Ishii *et al.*, Opt. Lett. **30**, 567 (2005).
12. I. Jovanovic *et al.*, Opt. Lett. **30**, 1036 (2005).
13. S. Witte *et al.*, Opt. Express **13**, 4903 (2005).
14. V. V. Lozhkarev *et al.*, Opt. Express **14**, 446 (2006).
15. O. V. Chekhlov *et al.*, Opt. Lett. **31**, 3665 (2006).
16. D. Kraemer *et al.*, J. Opt. Soc. Am. B **24**, 813 (2007).
17. J. H. Kelly, L. J. Waxer, V. Bagnoud, I. A. Begishev, J. Bromage, B. E. Kruschwitz, T. J. Kessler, S. J. Loucks, D. N. Maywar, R. L. McCrory, D. D. Meyerhofer, S. F. B. Morse, J. B. Oliver, A. L. Rigatti, A. W. Schmid, C. Stoeckl, S. Dalton, L. Folnsbee, M. J. Guardalben, R. Jungquist, J. Puth, M. J. Shoup III, D. Weiner, and J. D. Zuegel, J. Phys. IV France **133**, 75 (2006).
18. N. Forget *et al.*, Opt. Lett. **30**, 2921 (2005).
19. I. N. Ross, G. H. C. New, and P. K. Bates, Opt. Commun. **273**, 510 (2007).
20. A. V. Okishev and J. D. Zuegel, Appl. Opt. **43**, 6180 (2004).
21. L. B. Glebov *et al.*, in *Laser Weapons Technology III*, edited by W. E. Thompson and P. H. Merritt (SPIE, Bellingham, WA, 2002), Vol. 4724, pp. 101–109.
22. A. V. Okishev, C. Dorrer, V. I. Smirnov, L. B. Glebov, and J. D. Zuegel, Opt. Express **15**, 8197 (2007).
23. V. Bagnoud, M. J. Guardalben, J. Puth, J. D. Zuegel, T. Mooney, and P. Dumas, Appl. Opt. **44**, 282 (2005).